

Inhomogeneous activity enhances density phase separation in active model B

Ajeya Krishna* and Shradha Mishra†

Indian Institute of Technology (BHU), Varanasi, U.P. India - 221005

I. ABSTRACT

We study the binary phase separation in active model B, on a two-dimensional substrate with inhomogeneous activity. Activity is introduced with a maximum value at the center of the box and spread as a Bivariate-Gaussian distribution as we move away from the center. The system is studied for three different intensities of the distribution. Towards the boundary of the box, activity is zero or the model is similar to the passive model B. We start from the random homogeneous distribution of density of particles, system evolve towards a structured distribution of density. With time, density starts to phase separate with maximum density at the center of the box and decreases as we move away from the center of the box. The width of the density profile at the center increases as a power law with respect to time and reaches a maximum at the late time. The power law exponent increases with an increase in the intensity of the activity. Hence our result shows the response of density in an active binary system with respect to the patterned substrate. It can be used to design the devices useful for the trapping and segregation of active particles.

II. INTRODUCTION

Ranging from small organisms like bacteria [1], algae to higher organisms like fish [2], birds [3], animals self-organizes themselves to form complex structures [4]. This topic has been under active research for the past decade [5]. Emergence of meso-scale[6–9] turbulent motion was a forward step in research on non-equilibrium biological systems. Dynamics of active colloidal particles such as natural microorganisms like bacteria or algae [4, 10], or synthetic swimmers, active Brownian particles (ABP) [11–15] described by having a non-trivial dependence of active current to the local curvature of the underlying density profile. This leads to an activity term in standard binary phase separation in equilibrium system or also called as passive model B [16–18]. The corresponding active model is called as active model B (AMB) [19]. The study of passive model B [16–18] is useful to understand the phase separation in equilibrium binary systems [16, 17], whereas active

*ajeya.krishnap.phy17@iitbhu.ac.in

†smishra.phy@itbhu.ac.in

model B, gives the understanding of phase separation in many natural and biological systems. Also, many artificially designed active Janus particles in the lab are also useful candidates for technological and pharmaceutical applications [20–22]. Active Brownian particles predominantly show short-range steric repulsion [23]. The presence of activity shows fascinating behavior like coherent motion, phase separation without any external parameter or quenching in temperature [4, 24]. The phase separation of systems with self-propelled particles (active particles) is studied numerically [23, 25–27] and to some extent in experimental studies [28, 29].

In this study, we consider a conserved scalar order parameter ϕ which is linearly associated to the local density of the particles. The motivation of selecting a scalar order parameter is Model B [19, 30]. The resulting phase-separation kinetics of passive colloidal particles is best described by mean field theories involving a conserved scalar order parameter ϕ (continuous local density parameter). Simplifying the free energy to quadratic polynomial in ϕ using general diffusion mechanisms, gives a theory of “Model B”. Model B or ϕ^4 field theories are the simplest form of Cahn-Hilliard equation [16–18].

The kinetics of phase separation of passive and active systems are extremely distinct but coarse-graining of active systems at large scale demonstrates some relation between the two cases. The relation was first observed in models of swimming bacteria with discrete reorientations [31] and later extended to ABPs [32].

In our model, we are adding a non-integrable gradient term to passive Model B [16–18]. The added gradient term simply breaks detailed balance in Passive Model B, which suggest that active model B cannot be derived from a free-energy functional [19]. In this active model, we add $\lambda|\nabla\phi|^2$ term to the derivative of free-energy functional or simply chemical potential. The λ here determines the strength of activity in the system. In previous studies, [19, 33], the activity λ is considered a constant value or uniform over the system. In this work, we consider λ inhomogeneous in space and take it as Bivariate-Gaussian distributed in the system. We consider a two-dimensional square box with periodic boundary condition, where the activity is chosen maximum at the center of the box and decay as a Bivariate-Gaussian distribution as we go away from the center. The system is studied for three different values of maximum intensity at the center. We call the model as inhomogeneous active model B (IAMB). For comparison we also studied the constant activity model, where λ remains constant in the whole system. Below we report the results of steady state and kinetics of IAMB. We observed that on the increasing activity at the center of the box, lead to trapping of the particles at the center, hence higher the activity more the value of local density. We later studied the growth kinetics of density in the middle of the box for three different intensities

and find the density grow as a power law with time. The power law exponent varies from 2/3 to 3/4 as we go from low to high intensity in the system.

The rest of the article is divided in the following manner. In next section III we first describe our model then in section IV we discuss our results in detail and finally conclude in section V.

III. MODEL AND NUMERICAL DETAILS

We consider a conserved scalar order parameter field $\phi(\mathbf{r}, \mathbf{t})$ at position \mathbf{r} and time t in two dimensions. The variable ϕ is linearly related to the local number density $\rho(r, t)$ of active particles by the transformation $\phi = \frac{(2\rho - \rho_H - \rho_L)}{(\rho_H - \rho_L)}$, where ρ_H and ρ_L are the high and low local densities co-existing phases respectively. The dynamical equation for rate of change of ϕ is given by continuity equation [34, 35]:

$$\frac{\partial \phi}{\partial t} = -\nabla \cdot J \quad (1)$$

$$J = -\nabla \mu \quad (2)$$

$$\mu = -\phi + \phi^3 - \nabla^2 \phi + \lambda |\nabla \phi|^2 \quad (3)$$

The expression in eq. 1 represents the conservation of ϕ and the expression in eq. 2 expresses the relation between the mean current J and the non-equilibrium chemical potential μ . The mean current J is proportional to the negative gradient of the chemical potential μ .

The chemical potential $\mu = \mu_0 + \mu_1$ is the sum of bulk and gradient contributions. In equilibrium μ can be obtained by the variation of free energy functional. The bulk part μ_0 can be obtained from the polynomial terms in the standard ϕ^4 free energy functional, $\mu_0 = \frac{\delta}{\delta \phi} f_0$, where $f_0 = -\frac{\phi^2}{2} + \frac{\phi^4}{4}$. Hence, $\mu_0 = -\phi + \phi^3$.

The gradient term μ_1 has two terms, $\mu_1 = \mu_1^p + \mu_1^a$. The passive gradient term is $\mu_1^p = -\nabla^2 \phi$, which can be obtained by variation of gradient term in Landau-Ginzburg free energy functional [36]. The μ_1^a is the simplest addition to chemical potential, that cannot be derived from a free-energy functional. The active gradient term is the same as obtained for active model B, $\mu_1^a = \lambda |\nabla \phi|^2$ [19]. In our present study it is *inhomogeneous* λ , instead of constant value. We write λ as Bivariate-Gaussian Distribution [37] which is given as eq. 4 ,

$$\lambda(x, y) = \lambda_0 \times \frac{1}{2\pi\sigma_X\sigma_Y\sqrt{1-\rho^2}} \exp\left(-\frac{1}{2}\left[\frac{(x-\mu_X)^2}{\sigma_X} - \frac{2\rho(x-\mu_X)(y-\mu_Y)}{\sigma_X\sigma_Y} + \frac{(y-\mu_Y)^2}{\sigma_Y}\right]\right) \quad (4)$$

In eq. 4, μ_X, μ_Y are the mean along x and y directions respectively. In our case it is the center of the system. $\sigma_X = \sigma_Y = \sigma$ represents variance along x and y directions. In our case it is $\frac{1}{4}$ * (size of system). In eq. 4, ρ refers to correlation of distribution in x and y . In our case, there is no correlation i.e., $\rho \approx 0$. x and y in eq. 4, represents x and y co-ordinates of the system. λ_0 determines the maximum intensity of the distribution.

We studied the model for three different cases $G = [\lambda_0, \sigma]$: $G = [1.0, 32]$, $G = [2.0, 32]$, $G = [3.0, 32]$, where first number in the square bracket represent the maximum intensity at the center and second number denote the spread or variance of the distribution. In Fig., 1 we have graphically visualized the Bivariate-Gaussian distribution in color plot.

Intensity plots for diferent λ_0 :- Here, we graphically represent the different intensities of Gaussian distribution of activity. We included 2D plots in Fig. 1, in which center peak has highest value and value decreases confirming the Gaussian distribution.

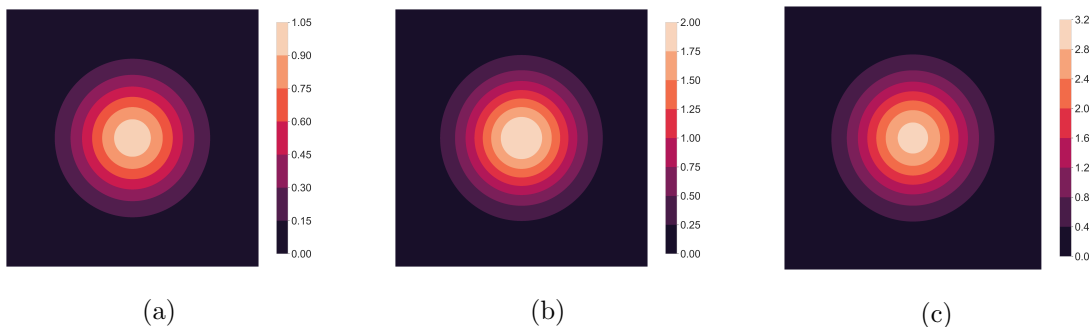


FIG. 1: Graphical representation of the distribution $\lambda(x, y)$. (a) $\lambda_0 = 1$, i.e., $G = [1.0, 32]$. (b) $\lambda_0 = 2$, i.e., $G = [2.0, 32]$. (c) $\lambda_0 = 3$, i.e., $G = [3.0, 32]$. Color bar represents the local intensity of activity.

Numerical Details: We have performed numerical analysis on our model using numerical methods to solve differential eqs. 1, 2, 3. We randomly initialized ϕ and calculated chemical potential (μ) which is given as in eq. 3. Computing chemical potential (μ), we can calculate flux(J) which is given as in eq. 2. Then the ϕ is updated using flux (J) from eq. 2 and inserting it in eq. 1. The stochastic differential equations of this model were solved by using Euler's numerical method [38]. The essential parameters we have considered are, $dx = 1.0$, $dy = 1.0$, $dt = 0.01$. We considered a critical system i.e., number of higher density particles equals number of lower density particles. The system was iterated for 5000 times i.e., $t = 5000$. The scalar order parameter

$\phi(r, t)$ was randomly initialized, with highest value as 0.5 and lowest value as -0.5 . The mean and variance of this distribution were 0.0 and 0.5 respectively. The system size is 128×128 . Periodic Boundary Conditions(PBC) were used in this model. In the case of Bivariate-Gaussian distribution of λ , the essential parameters are μ_X , μ_Y , σ , and λ_0 . Parameters μ_X and μ_Y determines the mean of the distribution. In this model, center of system is considered as origin, so $\mu_X = 0$ and $\mu_Y = 0$. Parameters σ determines the variance of our model. In our model, variance is $\frac{1}{4}$ *(size of system) which is 32. So variance along x and y directions $\sigma = 32$. Parameter λ_0 determines the intensity of distribution. Our system is studied for 3 different intensities $\lambda_0 = 1, 2, 3$.

IV. RESULTS

Now we discuss our results in detail: We integrate the nonlinear partial differential equation for local density with mean density $\phi_0 = 0.0$ for three different cases $G = [1.0, 32]$, $G = [2.0, 32]$, $G = [3.0, 32]$. First we consider active model B with constant activity parameter (AMB). After that we consider the three different intensities of Gaussian distribution in the model.

Active model B (AMB) :- In this section, we will discuss the results of active model B. This model has a constant activity ($\lambda = 1.0$) all over the system with box size $L = 64$. This study is preformed to understand the comparison between the constant activity parameter (AMB) and Gaussian distribution of activity parameter (IAMB). We observe interesting difference in the kinetics of domain formation and steady state structure of domains. Fig. 2 shows the real space snapshot of density at time steps = 0, 1000, 2000, 3000, 4000, 5000. Starting from random homogeneous density, as time progress, high density regions starts to phase separate and phase separation happens with the formation of isolated domains [19]. The size of the domains increases with time.

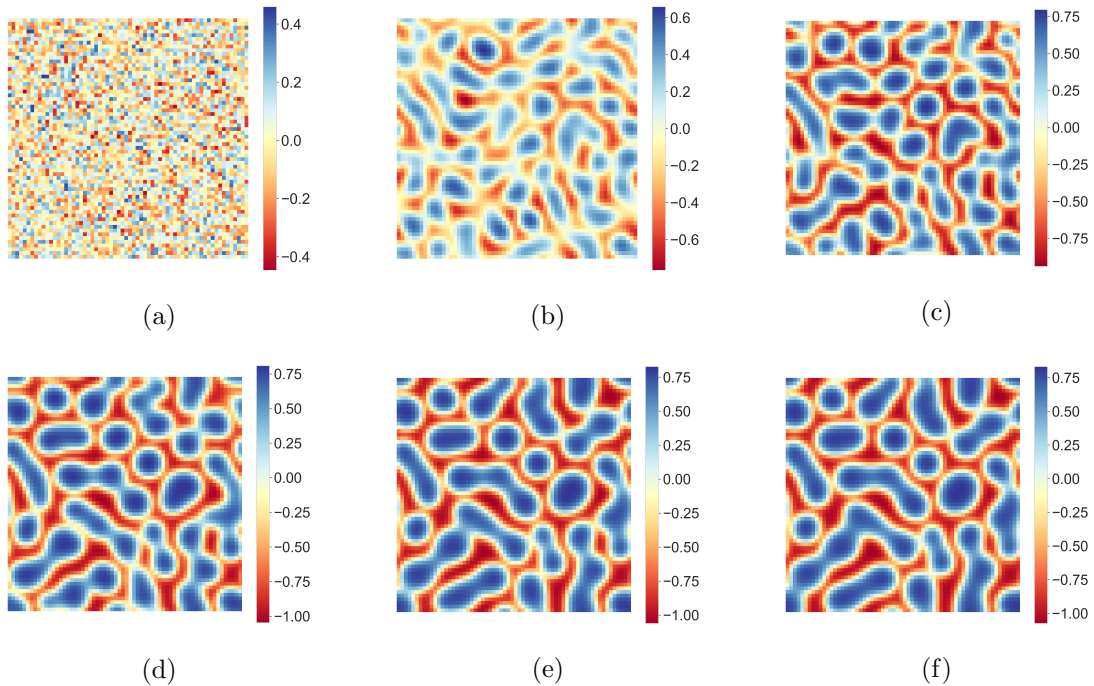


FIG. 2: Density evolution snapshots of the Active model B . (a) at $t=0$, (b) at $t=1000$, (c) at $t=2000$, (d) at $t=3000$, (e) at $t=4000$, (f) at $t=5000$. The color bar represents the value of local density ϕ .

A. Time evaluation of density for inhomogeneous activity (IAMB)

In this section, we will discuss the results of Gaussian activity of intensity, *i.e.*, $G = [1.0, 32]$, $G = [2.0, 32]$, $G = [3.0, 32]$. In this case at the middle of the box, strength of the activity is highest and as we go away it spreads like a normal distribution. When we include the distribution of activity, we observe that the high density at the center, where there is higher activity. Accumulation of particles decreases as we move away from the center of the system. When we enter into zero activity space, we can observe that particles form connected domains from walls of system to boundary of activity distribution. These connected domain structure is result of the passive phase separation mechanism or passive model B [16–18]. Density of both particles are conserved in this system. There are some droplets formation at the boundary of the distribution of constant activity, which is a characteristics of active model B. Fig. 2.

Case 1: Gaussian Distribution of activity with $\lambda_0 = 1$: In this case we consider the lowest intensity distribution i.e., ($\lambda_0 = 1$) which is represented graphically in Fig. 1a. In Fig. 3, we attached snapshots of density evolution.

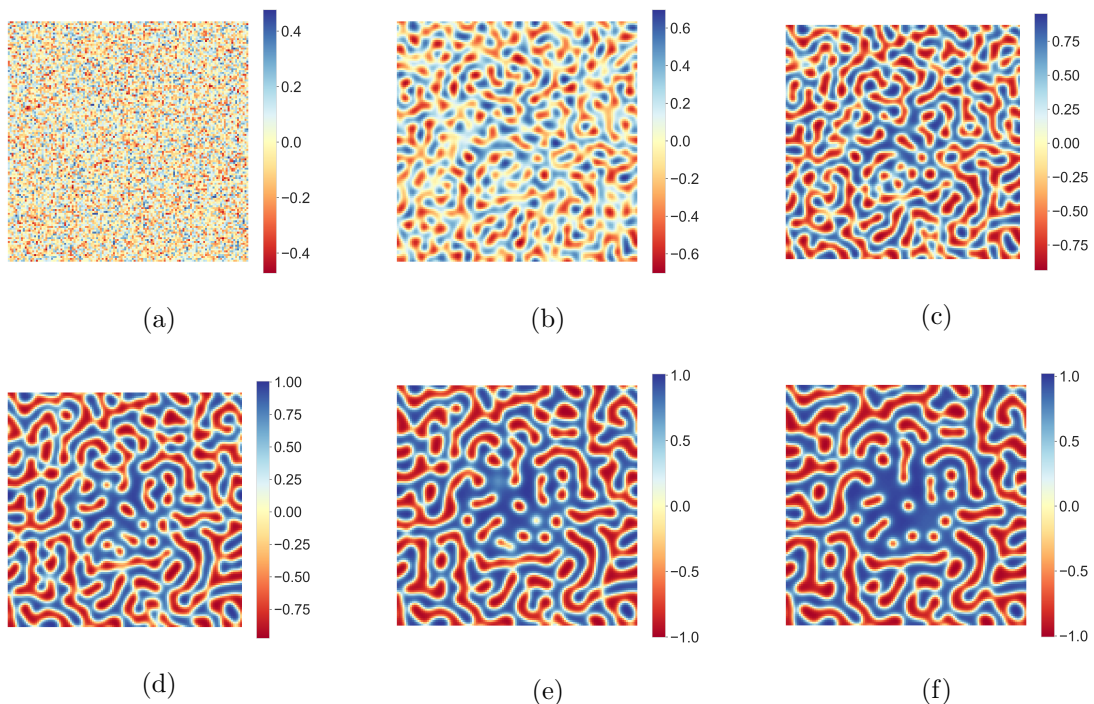


FIG. 3: Evolution snapshots of the active model B with Gaussian distribution of activity with $\lambda_0 = 1.0$. (a) at $t=0$, (b) at $t=1500$, (c) at $t=2500$, (d) at $t=3500$, (e) at $t=4000$, (f) at $t=5000$. The color bar have the same meaning as in Fig. 2

In Fig. 3, we have snapshots of density evolution with time. When the intensity of distribution is $\lambda_0 = 1.0$, we observe small-scale accumulation of high density particles at the center of the box. In Fig. 3a, particles are randomly distributed in system, so we observe scattered density. With time, we can see the accumulation of higher density particles at the center of system. Droplets of lower density particles are also formed besides the accumulation of higher density particles in activity region.

Case 2: Gaussian Distribution of activity with $\lambda_0 = 2$: In this case we consider the intensity distribution which is represented graphically in Fig., 1b. In Fig. 4 we show snapshots of density evolution of the system.

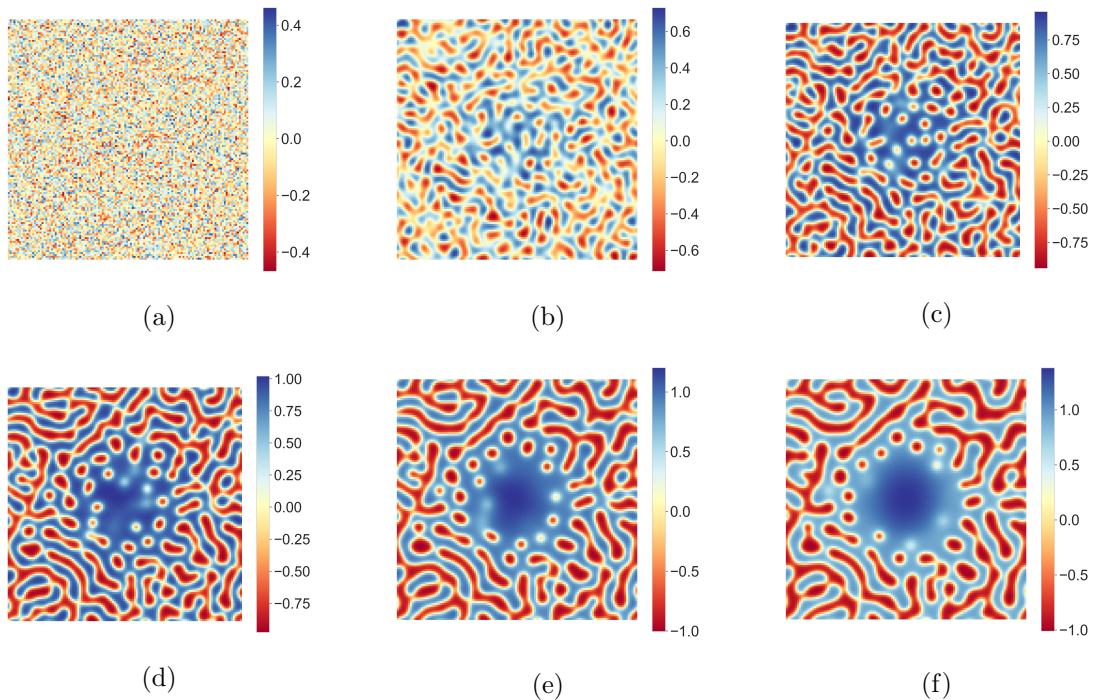


FIG. 4: Evolution snapshots of the active model B with Gaussian distribution of activity with $\lambda_0 = 2.0$. (a) at $t=0$, (b) at $t=1500$, (c) at $t=2500$, (d) at $t=3500$, (e) at $t=4000$, (f) at $t=5000$. The color bar have the same meaning as in Fig. 2

In Fig. 4 we can observe the evolution of the system. When the intensity of distribution is $\lambda_0 = 2.0$, we again observe more accumulation of particles at the center where there is maximum value for activity. Traversing from the center of system to the walls of system, there is decrease in particle accumulation and we observe lower density particles forms connected domains outside the activity domain. Droplets of lower density particles are also formed besides accumulation of higher density particles.

Case 3: Gaussian Distribution of activity with $\lambda_0 = 3$: In this case we consider the intensity distribution which is represented graphically in Fig. 1c. In Fig. 5 we show snapshots of density evolution of the system.

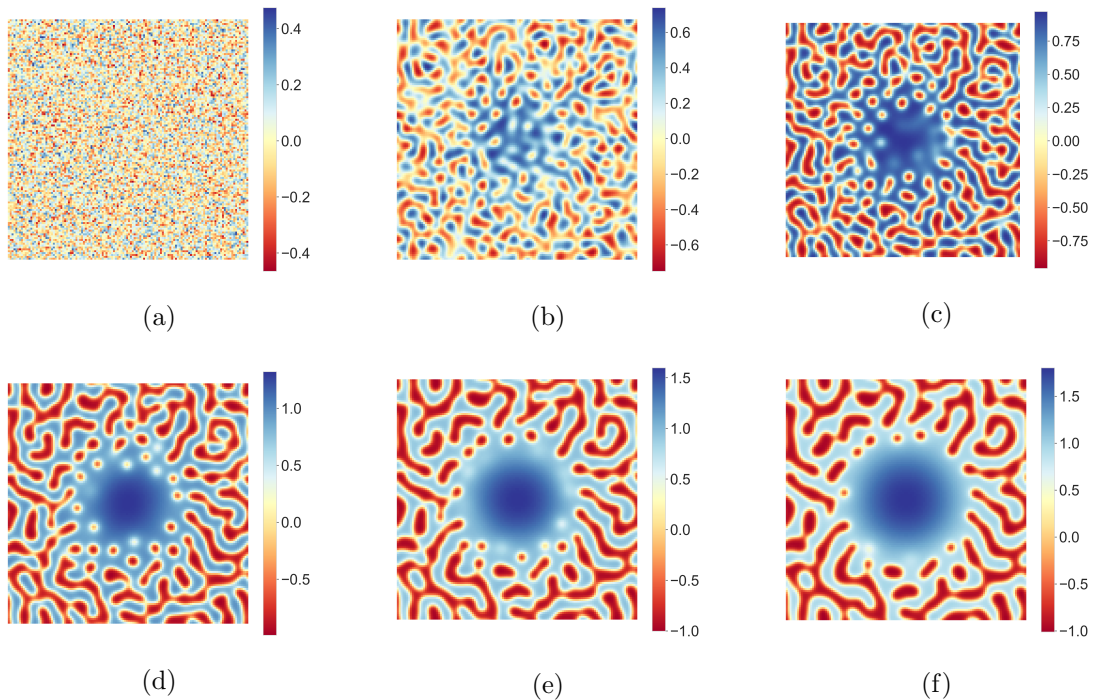


FIG. 5: Evolution snapshots of the active model B with Gaussian distribution of activity with $\lambda_0 = 3.0$. (a) at $t=0$, (b) at $t=1500$, (c) at $t=2500$, (d) at $t=3500$, (e) at $t=4000$, (f) at $t=5000$. The color bar have the same meaning as in Fig. 2.

In Fig. 5 we can observe the evolution of the system. When the intensity of distribution is $\lambda_0 = 3.0$ which is the highest intensity we considered. Here in this system we again observe the accumulation of higher density particles at the center where there is maximum value for activity. Very clearly at the center, there are no low density particles which convey us the accumulation of particle in high density region. Traversing from the center of system to walls of system, there is decrease in particle accumulation and we observe lower density particles form connected domains outside the activity domain. Droplets of lower density particles are also formed at the boundaries of active region besides accumulation of higher density particles at the center of the system.

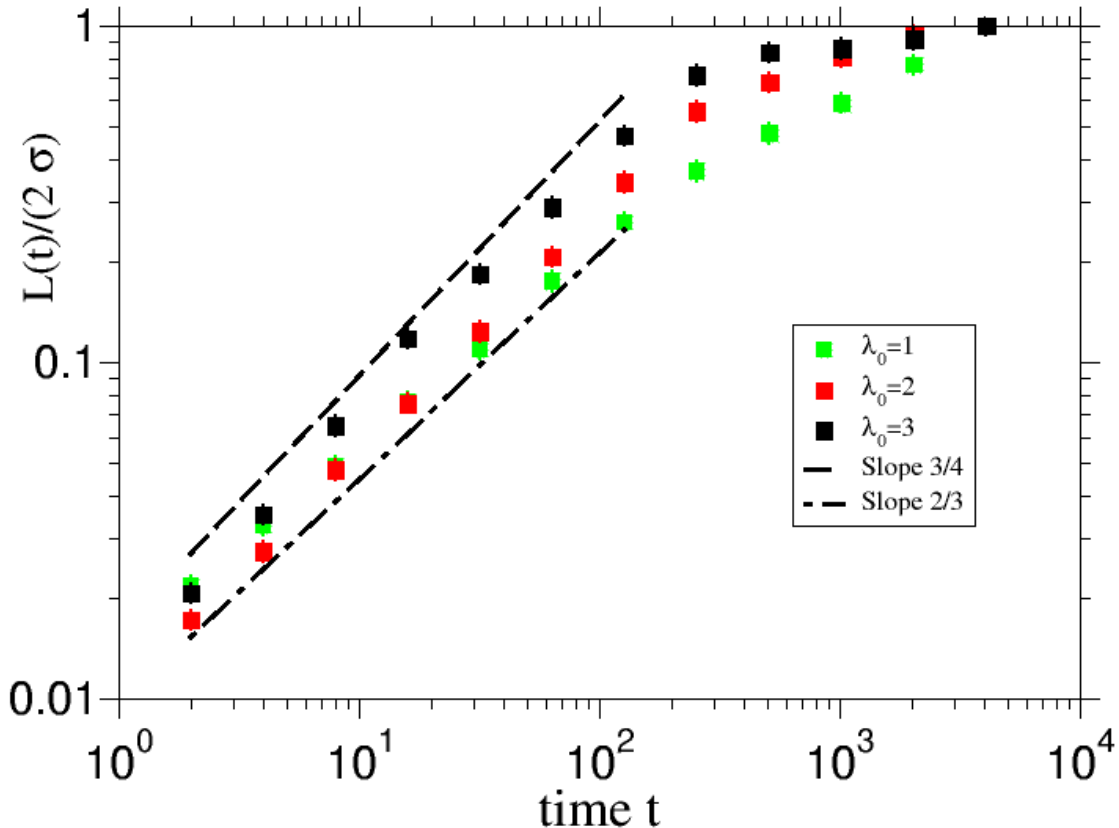


FIG. 6: Comparison Plot of $\frac{L(t)}{(2\sigma)}$ vs Time (t) for different intensities of distribution. The comparison is for scaled length i.e., $t = 5000$.

B. Kinetics of growing domains in high activity region

We now estimate the kinetics of growing high density domain at the center of the box, for different intensities $G = [1.0, 32]$, $G = [2.0, 32]$, $G = [3.0, 32]$. We measure the growth of high density domains at the center of the box in the following manner. We first change the continuous density field ϕ to binary density $\psi = +1$ if $\phi > \phi_0$ and $\psi = -1$ if $\phi < \phi_0$, then calculate the mean size of domains $L(t)$ of high density in the center of the box. Mean is calculated over 20 independent realisations. As time progress the domain size increases $L(t)$ at the middle of the box. We estimate the length of the growing domains at the center of the box and plot the scaled length $\frac{L(t)}{2\sigma}$ vs. time t for three different intensities. In Fig. 6, the plot is shown for the three cases. Very clearly growth is faster for larger intensities and saturates at late times. The $L(t)$ grows with time

as, $L(t) \simeq t^\alpha$, where $\alpha \sim 3/4$ to $2/3$ as we go from largest to smallest intensity in our model. Hence activity induces faster accumulation of particles in high activity region.

V. DISCUSSION

We have studied the steady state and dynamics of phase separation of active-particles: which experience the inhomogeneous activity on a two-dimensional substrate. Activity parameter is distributed as Bivariate-Gaussian distribution at the center of the system, with standard deviation of $\frac{1}{4}$ *(size of the system). Unlike model with constant activity parameter we have observed that accumulation of particles with variable densities are formed. The accumulation increases by increasing the intensity of distribution. In the region outside the distribution or away from the distribution, density phase separation is same as for passive model B. [16–18]

We also estimated the growth of high density domains in the center of the box with time. The domain of high density in the region of high activity grow as a power law with time. The power law exponent increases with increasing intensity of activity distribution.

Hence our study gives an interesting steady state of density phase separation of active particles on a inhomogeneous patterned substrate and it can be useful to understand the trapping and transport of active particles in inhomogeneous systems. A detail understanding of density phase separation is required to understand the mechanism of density phase separation in the inhomogeneous system.

VI. REFERENCES

-
- [1] J. T. Bonner, Proc. Natl. Acad. Sci. U.S.A. 95, 9355 (1998).
 - [2] J. K. Parrish and W. M. Hammer (eds), Animal Group in Three Dimensions (Cambridge: Cambridge University Press) (1997).
 - [3] D. Chen , Y. Wang, G. Wu, M. Kang, Y. Sun, and W. Yu, Chaos29, 113118 (2019).
 - [4] M. C. Marchetti, J. F. Joanny, S. Ramaswamy, T. B. Liverpool, J. Prost, Madan Rao, and R. Aditi Simha Rev. Mod. Phys. 85, 1143 (2013).
 - [5] H. H. Wensink, J. Dunkel, S. Heidenreich, K. Drescher, R. E. Goldstein, H. Lowen, and J.M Yeomans, Proc. Natl. Acad. Sci. U.S.A. , 109(36), 14313 (2012).
 - [6] C. Dombrowski, Cisneros, S. Chatkaew, R. E. Goldstein, J. O. Kessler, Phys. Rev. Lett. 93, 098103 (2004).

- [7] A. Sokolov, I. S. Aranson, J. O. Kessler, R. E. Goldstein, *Phys. Rev. Lett.* 98, 158102 (2007).
- [8] L. H. Cisneros, R. Cortez, C. Dombrowski, R. E. Goldstein, J. E. Kessler, *Exp. Fluids* 43, 753 (2007).
- [9] C. W. Wolgemuth, *Biophys J* 95, 1574 (2008).
- [10] M. E. Cates, *Rep. Prog. Phys.* 75, 042601 (2012).
- [11] Jonathan R. Howse, Richard A. L. Jones, Anthony J. Ryan, Tim Gough, Reza Vafabakhsh, and Ramin Golestanian, *Phys. Rev. Lett.* 99, 048102 (2007)
- [12] S. J. Ebbens and J. R. Howse, *Soft Matter* 6, 738 (2010).
- [13] S. Thutupalli, R. Seemann and S. Herminghaus, *New J. Phys.* 13, 073021 (2011).
- [14] G. Volpe, I. Buttinoni, D. Vogt, H. Kümmerer and C. Bechinger, *Soft Matter* 7, 8815 (2011).
- [15] J. Palacci, S. Sacanna, A. P. Steinberg, D. J. Pine and P. M. Chaikin, *Science* 339, 940 (2013).
- [16] Ken A Hawick, Daniel P Playne. Modelling and Visualizing the Cahn-Hilliard-Cook Equation, Technical Report CSTN-049, 155 (2008).
- [17] J. W. Cahn and J. E Hilliard. *Chem. Phys.* 28, 267 (1958).
- [18] J. W. Cahn and J. E. Hilliard *J. Chem. Phys.* 31, 688 (1959).
- [19] R. Wittkowski, A. Tiribocchi, J. Stenhammar, R. J. Allen, D. Marenduzzo, and M. E. Cates, *Nat. Comm.* 5, 4351 (2014).
- [20] S. Pattanayak, R. Das, M. Kumar, and Shradha Mishra, *Eur. Phys. J. E* 42, 62 (2019).
- [21] P. Malgaretti and H. Stark, *J. Chem. Phys.* 146, 174901 (2017).
- [22] Bao-quan Ai, Qiu-yan Chen, Ya-feng He, Feng-guo Li, and Wei-rong Zhong *Phys. Rev. E* 88, 062129 (2013).
- [23] P. Dolai, A. Simha, and S. Mishra, *Soft Matter*, 14(29), 6145 (2018).
- [24] S. Ramaswamy, *Annual Review of Condensed Matter Physics*, 1323 (2010).
- [25] J. P. Singh and S. Mishra, *Physica A: Statistical Mechanics and its Applications* 544, 123530, (2020).
- [26] Y. Fily and M. C. Marchetti, *Phys. Rev. Lett.* 108, 235702 (2012).
- [27] J. Stenhammar, A. Tiribocchi, R. J. Allen, D. Marenduzzo and M. E. Cates, *Phys. Rev. Lett.* 111, 145702 (2013).
- [28] Ivo Buttinoni, Julian Bialké, Felix Kümmel, Hartmut Löwen, Clemens Bechinger, and Thomas Speck, *Phys. Rev. Lett.* 110, 238301 (2013).
- [29] Quan-Xing Liu, Arjen Doelman, Vivi Rottschäfer, Monique de Jager, Peter M. J. Herman, Max Rietkerk, and Johan van de Koppel, *Proc. Natl Acad. Sci. USA* 110, 11910 (2013).
- [30] Sanjay Puri, Vinod Wadhawan. *Kinetics of Phase Transitions*, CRC Press (2009).
- [31] J. Tailleur and M. E. Cates, *Phys. Rev. Lett.* 100, 218103 (2008).
- [32] M. E. Cates and J. Tailleur, *Europhys. Lett.* 101, 20010 (2013).
- [33] R Das, S Mishra, S Puri, *EPL* 121 37002 (2018).
- [34] A. Fick, *Annalen der Physik* 170, 59 (1855).
- [35] A. Paul, T. Laurila, V. Vuorinen, S.V. Divinski. *Fick's Laws of Diffusion*. In: *Thermodynamics, Diffusion and the Kirkendall Effect in Solids*. Springer, Cham (2014).

- [36] Paul M Chaikin, T. C. Lubensky, Principles of condensed matter physics, Cambridge University Press (1995).
- [37] N Balakrishnan, and Chin-Diew Lai. Continuous Bivariate Distributions, Springer-Verlag Press (2009).
- [38] Richard W. Hamming, Numerical Methods for Scientists and Engineers, Mc-Graw-Hill (1973).